Estimation of the spatial profile of neuromodulation and the temporal latency in motor responses induced by focused ultrasound brain stimulation

Hyungmin Kim[a,b], Stephanie D. Lee[a], Alan Chiu[a], Seung-Schik Yoo[a] and Shinsuk Park[b]

This study investigates the spatial profile and the temporal latency of the brain stimulation induced by the transcranial application of pulsed focused ultrasound (FUS). The site of neuromodulation was detected using 2-deoxy-2-[^{18}F]fluoro-D-glucose PET immediately after FUS sonication on the unilateral thalamic area of Sprague–Dawley rats. The latency of the stimulation was estimated by measuring the time taken from the onset of the stimulation of the appropriate brain motor area to the corresponding tail motor response. The brain area showing elevated glucose uptake from the PET image was much smaller (56±10% in diameter, 24±6% in length) than the size of the acoustic focus, which is conventionally defined by the full-width at half-maximum of the acoustic intensity field. The spatial dimension of the FUS-mediated neuromodulatory area was more localized, approximated to be full-width at 90%-maximum of the acoustic intensity field. In addition, the time delay of motor responses elicited by the FUS sonication was 171±63 (SD) ms from the onset of sonication. When compared with latencies of other nonultrasonic neurostimulation techniques, the longer time delay associated with FUS-mediated motor responses is suggestive of the nonelectrical modes of neuromodulation, making it a distinctive brain stimulation method. *NeuroReport* **25:475–479 © 2014 Wolters Kluwer Health | Lippincott Williams & Wilkins.**

NeuroReport 2014, **25**:475–479

Keywords: focused ultrasound, neuromodulation, ultrasound

[a]Department of Radiology, Brigham and Women's Hospital, Harvard Medical School, Boston, Massachusetts, USA and [b]Department of Mechanical Engineering, Korea University, Seoul, Korea

Correspondence to Seung-Schik Yoo, PhD, MBA, Department of Radiology, Brigham and Women's Hospital, Harvard Medical School, 75 Francis Street, Boston, MA 02115, USA
Tel: +1 617 732 9464; fax: +1 617 732 9185; e-mail: yoo@bwh.harvard.edu

Received 21 October 2013 **accepted** 5 December 2013

Introduction

The research to utilize ultrasound as a novel neuromodulatory tool has been gaining momentum. Ultrasound has been used to modulate the activities of neuromuscular tissues, for example the stimulation of nerve and muscle fibers in frog hearts [1], the excitation of auditory nerve responses in a craniotomized cat brain [2], the modification of neuronal action potential in excised rodent brains [3], and the stimulation of motor areas in intact rodent brain tissues [4]. With the accumulation of evidence for these various neuromodulatory effects, the scope of the potential therapeutic use of ultrasound has broadened.

By converging the acoustic energy to a specific location transcranially, focused ultrasound (FUS) techniques have distinguished spatial specificity and penetrability as a noninvasive therapeutic modality [5], rendering a new breed of applications, such as functional neurosurgery [6] and brain tumor ablation [7]. When administered in bursts of short pulses, FUS has been shown to reversibly excite or suppress the region-specific brain functions in rabbits [8] and rodents [9]. In addition, the administration of this neuromodulatory FUS to the thalamic area of the rodent brain altered the level of extracellular neurotransmitters (γ-aminobutyric acid, dopamine, and serotonin) [10,11] and shortened the emergence time from anesthesia [12]. Recently, the stimulation of rodent cranial nerves yielded the potential use of FUS in the functional modulation of the peripheral nervous system [13].

Despite the diverse neuromodulatory effects of FUS, the spatial and temporal characteristics of FUS-mediated neuromodulation, which would form the basis for its potential therapeutic use, have not been examined in detail. In this study, the spatial dimension of FUS-mediated neuromodulation was estimated by imaging the changes in glucose metabolism of the brain using 2-deoxy-2-[^{18}F]fluoro-D-glucose PET (^{18}F-FDG-PET). The time latency in the motor response, as detected by tail twitching, with respect to the FUS stimulation of the appropriate motor area of the brain, was also investigated.

Materials and methods

This study was carried out under the approval of the Harvard Medical Area Standing Committee on Animals.

0959-4965 © 2014 Wolters Kluwer Health | Lippincott Williams & Wilkins

DOI: 10.1097/WNR.0000000000000118

Sonication setup

Two waveform generators that were serially connected (33210A; Agilent, Santa Clara, California, USA) created a train of pulsed electrical signal waves that determined the fundamental frequency (FF), pulse-repetition frequency (PRF), tone-burst duration (TBD), sonication duration (SD), and acoustic intensity (AI), whereby the duty cycle (DC) was determined by the product of the PRF and TBD (detailed methods are described by Yoo *et al.* [8]). A linear power amplifier (240L; ENI Inc., Rochester, New York, USA) amplified the electrical signals and transmitted the signal to an air-backed, single-element FUS transducer (spherical segmented in shape, 6 cm in diameter, 7 cm in radius of curvature, 350 kHz FF). The acoustic characteristics, such as dimension of acoustic focus and intensity, generated by the FUS transducer were measured using a needle-type hydrophone mounted to a field mapping system (procedures described by Kim *et al.* [14]).

Estimation of spatial profiles of FUS-mediated neuromodulation

Animal preparation and sonication parameters

Male Sprague–Dawley rats ($n = 7$, 279 ± 15 g) were anesthetized with isoflurane (3.5% for induction and 1.5% for maintenance, all in 95% oxygen at a flow rate of 1 l/min) by a nose cone. The fur over the rat's head was removed to maintain acoustic transmission through the scalp. After placing a catheter (24 G) through the tail vein for ^{18}F-FDG injection, the rat was immobilized with a stereotactic frame (SRP-AR; Narishige, Tokyo, Japan). The transducer was then coupled to the rat's head by a cone-shaped degassed water bag with hydrogel applied onto the interface between the scalp and the bag. Under geometry-based, stereotactic optical guidance [11], the sonication target was placed onto the unilateral thalamic area. The hemispheric side of the sonication target was randomized and balanced across the animals (left: $n = 3$, right: $n = 4$). Immediately after the ^{18}F-FDG injection, the sonication commenced and continued for 40 min. The same stimulatory sonication parameters (0.5 ms TBD, 1 kHz PRF, 300 ms SD, 2 s of interstimulus intervals) that elicited tail movement in rats [15] were adopted, although a lower AI (3 W/cm^2 I_{spta}; compared with 4.5 W/cm^2 I_{spta} in the study by Kim *et al.* [15]) was used to comply with the upper limit of ultrasound physiotherapy equipment set by the International Electrotechnical Commission (IEC) [16].

Detection of FUS-mediated metabolic changes using ^{18}F-FDG-PET scanning

After the sonication, the animal was removed from the sonication stage and was subjected to PET scanning (eXplore Vista; GE Healthcare, Waukesha, Wisconsin, USA). The reconstructed PET data consisted of 61 images of 175×175 in matrix size with 68×68 mm^2 in the field-of-view, resulting in voxel dimensions of $0.39 \times 0.39 \times 0.78$ mm^3, and the pixel-by-pixel average standardized uptake value (SUV) was calculated at 1 h after injection to detect the level of glucose metabolic activities in the brain [14].

To detect the brain area showing an elevated SUV level because of sonication, the average SUV from the unsonicated area (which was 6×6 mm^2, marked as a black rectangle in Fig. 1a), which lies contralateral to the site of sonication, was measured to establish the baseline level of metabolic activity. Then, the pixels showing a greater SUV were located transversely and longitudinally along the sonication path (shown as arrows in Fig. 1a) to estimate the size of the stimulation profile.

Estimation of temporal delay of FUS-mediated neuromodulation

Animal preparation and sonication parameters

Male Sprague–Dawley rats ($n = 17$) were anesthetized with an intraperitoneal injection of a ketamine/xylazine mixture of 80 : 10 mg/kg. On the basis of the functional atlas obtained by transdural electrical stimulation on the motor cortex of the rat [17], the specific brain area for tail movement (2 mm posterior to the Bregma along the midline) was targeted by the optical guidance system [11] (Fig. 2).

The same set of sonication parameters (350 kHz FF, 0.5 ms TBD, 1 kHz PRF, 300 ms SD) as the PET experiment was initially used, although an increased AI (4.5 W/cm^2 I_{spta}) was used briefly to elicit definite tail movement in the rats [15]. After localizing the area that responded to the stimulation, the AIs were changed to determine the minimum AIs (3.5 ± 1.5 W/cm^2 I_{spta}) inducing the motor responses, while varying the TBDs (0.25, 0.5, 1, 2, 3, and 5 ms) at three different DCs ($n = 9$, 287 ± 36 g for 30% DC; $n = 9$, 278 ± 23 g for 50% DC; $n = 5$, 294 ± 21 g for 70% DC). The parameter set used for each session was randomized and balanced across the animals. There were no significant differences in animal weights between any of the groups in comparison [one-way analysis of variance, $F(2,20) = 0.53$, $P = 0.597$].

Detection of FUS-mediated motor response

The elicited tail movement was detected using an external motion sensor (Piezo Electric Pulse Transducer, MLT1-1010/D; AD Instruments, Colorado Springs, Colorado, USA) and recorded (PowerLab 8/30 and LabChart 7; AD Instruments) at a sampling rate of 1 kHz with a low-pass filter (3 Hz) to reduce the contribution of the heart and respiratory signals. For the threshold criterion of detecting the tail movement, two times the SD (2σ) of the resting-state signals was chosen over the three times (3σ) used in a previous study [18] because of its higher sensitivity to detect subtle movements. The response time was defined by the time difference between the onset of FUS sonication and

Fig. 1

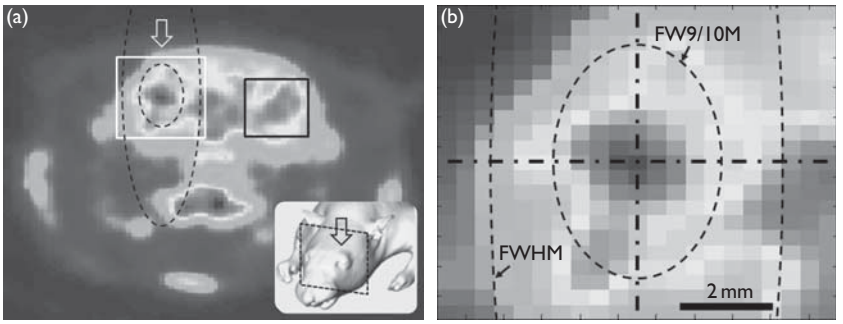

(a) An exemplar PET image from one animal with an illustration of sonication (inset). The arrows indicate the direction of the sonication path. A region-of-interest (marked in a black rectangle) was placed on the opposite side of the sonicated hemisphere to estimate the baseline standardized uptake value signal level. (b) A close-up look near the acoustic focus. The longitudinal (vertical) and transversal (horizontal) orientations to the sonication path are shown by dashed–dotted lines. The contours of the conventional acoustic focus (denoted as 'FWHM') and the approximated neuromodulatory area according to the group-based analysis (denoted as 'FW9/10M') are shown by dashed lines. Note that the 'FW9/10M' of the acoustic intensity field, on the basis of the group-averaged estimation, occupied a much wider area than the stimulated area in the given example from one animal. FWHM, full-width at half-maximum.

Fig. 2

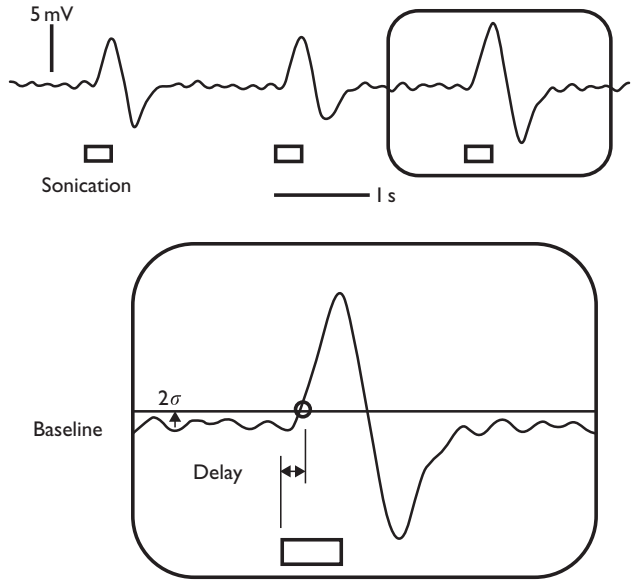

Recorded tail movement signal and the illustration of criterion (example shown from the single trial data from one animal, i.e. 2σ above the resting-state signal) for the measurement of response delay (inset). The duration of sonication (i.e. 300 ms) is represented by the rectangular boxes.

elicited tail movement, and averaged over a maximum of six events of sonication (Fig. 2).

Results

Neuromodulatory area

The resulting dimensions of the neuromodulatory area (exceeding the baseline signal level) were 3.7 ± 0.7 mm traversal to and 5.6 ± 1.3 mm longitudinal to the sonication path, which were $56 \pm 10\%$ in diameter and $24 \pm 6\%$ in length of the conventional size of the acoustic focus (i.e. 6.5 mm in diameter and 24 mm in length). This dimension of the neuromodulatory area was comparable with the full-width at 90%-maximum (denoted as 'FW9/10M') of the AI field. The aspect ratio (0.66), defined by the ratio between the length of the long and short axes of the neuromodulatory area, was higher when compared with that of the acoustic focus (0.27), suggesting that the actual site of neural activation was smaller but rounder in shape compared with the conventional 'cigar'-like elongated ellipsoidal shape. The results are also shown in Fig. 1b.

Motor response delay

The results of the motor response delay in FUS-mediated neuromodulation are summarized in Table 1. The gross average delay in FUS-mediated motor responses in rats was 171 ± 63 (SD) ms, with a minimum value of 54 ms and a maximum value of 435 ms across the tested sonication parameters (three DCs and six TBDs), with no significant difference among the different DCs for each TBD (one-way analysis of variance, $P > 0.05$).

Discussion

In this study, the spatial dimension of the neuromodulatory area and temporal delay in the motor response elicited by transcranial FUS were estimated. The size of the neuromodulatory area was found to be much smaller than the size of the acoustic focus, as defined traditionally by the full-width at half-maximum of the AI field. The average delay in motor response was measured to be 171 ± 63 (SD) ms from the onset of sonication.

Our data suggest that future studies involving FUS-mediated neuromodulation may need to consider that the stimulated area could be smaller than the size of the acoustic focus that is conventionally acknowledged in the field of acoustics. This result is supported by

Table 1 Delay in FUS-mediated motor responses at three DCs across six TBDs and one-way ANOVA result

	Delay in motor response (ms)			H_0: $\mu_a=\mu_b=\mu_c$		
TBD (ms)	(a) 30% DC	(b) 50% DC	(c) 70% DC	*d.f.*	*F*	*P*
0.25	159±23	208±27	136±13	2,12	3.512	0.063
0.5	145±23	180±22	135±24	2,13	1.343	0.295
1	192±55	183±19	190±21	2,16	0.024	0.977
2	218±92	182±19	134±27	2,13	1.470	0.266
3	182±45	207±13	135±29	2,14	1.451	0.267
5	189±30	155±18	141±27	2,12	1.132	0.355

The variations in delay are represented in SEs.
μ, population mean; ANOVA, analysis of variance; DC, duty cycle; *d.f.*, degree of freedom; FUS, focused ultrasound; H_0, null hypothesis; TBD, tone-burst duration.

previous findings in which small regions of cortical areas were selectively stimulated by FUS to specifically elicit only whisker, paw, or tail movements in rats [15,19]. The stimulatory effect occurred over roughly the size of the acoustic focus (on the basis of the full-width at half-maximum criterion, shown in Fig. 1b as a dashed line); a much greater area of the brain, perhaps covering almost the entire hemispheric brain functions in rodents, would have been affected by the sonication.

A smaller stimulatory area compared with the conventions used in acoustics may help to justify the utilization of FUS for neuromodulation studies aimed at human applications. For the transcranial application in humans, the use of a lower FF (e.g. 220 kHz, which is often used for a commercial image-guided FUS system [20]) is favored over higher frequencies because of its increased transmission through the skull. As the FF and the minimum achievable size of the acoustic focus are correlated inversely, the use of a lower frequency would increase the size of the acoustic focus. For example, the minimum diameter of the acoustic focus at 220 kHz, using sonication settings similar to the ones in this experiment, would be on the order of 7 mm (i.e. approximated to the wavelength of acoustic pressure wave, $d_{\min}$ = speed of sound in the water/frequency = 1484 m/s/220 kHz = 7 mm), which in turn increases the chance for the stimulation of nonspecific, broad brain areas. However, according to FW9/10M of the AI profile, the stimulatory area would be 3–4 mm in diameter, instead of 7 mm, which is small enough to elicit digit-specific finger sensation when the stimulation occurs at the somatosensory area of the human brain [21]. It is possible, however, that the inhomogeneous level of ^{18}F-FDG uptake by the inhomogeneous neural tissues under sonication, because of the use of small rodents, might have confounded the analysis in the present study. Therefore, further testing in larger animals, with more homogeneous brain regions for the given sonication focus, will yield a more accurate assessment of the effective spatial extent of stimulation by the FUS.

Factoring in the minimal time difference between the electromyography and the actual movement detection (on the order of 3 ms) [22], the average latency in motor response was much greater than those of nonultrasonic stimulation methods, for example 25 ms for intracortical microelectrode stimulation in rat [23], 26 ms for optogenetic stimulation in mice [22], and 10–20 ms for transcranial magnetic stimulation in human [24]. This finding suggests that the fundamental mechanism behind FUS-mediated neuromodulation may be different from those of nonultrasonic brain stimulation methods. One possible explanation is the involvement of astroglial systems that are sensitive to mechanical stimulation mediated by long calcium signaling [25]. Further studies need to be carried out to reveal definitive causes for the discrepancies.

The spatiotemporal characteristics of FUS-mediated neuromodulation identified in this study, that is the smaller stimulatory area and the prolonged delay in motor response, may be helpful in demystifying the fundamental mechanism underlying FUS-mediated neuromodulation. Further extension of this study to larger animals will be conducive to applying this technique to neurotherapeutics in humans, whereby the precise estimation of the anticipated neuromodulatory area and delayed effects are crucial.

Acknowledgements

This work was supported by grants from the National Institute of Health (R21 NS074124 to Yoo), the KIST Institutional Program (2E23031 to Yoo and Kim), and the National Research Foundation of Korea (Korean Ministry of Education, Science and Technology, 2010-0027294 to Park). The authors also thank an anonymous reviewer for the helpful and constructive comments.

Conflicts of interest

There are no conflicts of interest.

References

1 Harvey EN. The effect of high frequency sound waves on heart muscle and other irritable tissues. *Am J Physiol* 1929; **91**:284–290.
2 Foster KR, Wiederhold ML. Auditory responses in cats produced by pulsed ultrasound. *J Acoust Soc Am* 1978; **63**:1199–1205.
3 Tyler WJ, Tufail Y, Finsterwald M, Tauchmann ML, Olson EJ, Majestic C. Remote excitation of neuronal circuits using low-intensity, low-frequency ultrasound. *PLoS One* 2008; **3**:e3511.
4 Tufail Y, Matyushov A, Baldwin N, Tauchmann ML, Georges J, Yoshihiro A, *et al.* Transcranial pulsed ultrasound stimulates intact brain circuits. *Neuron* 2010; **66**:681–694.
5 Lele PP. A simple method for production of trackless focal lesions with focused ultrasound: physical factors. *J Physiol* 1962; **160**:494–512.
6 Martin E, Jeanmonod D, Morel A, Zadicario E, Werner B. High-intensity focused ultrasound for noninvasive functional neurosurgery. *Ann Neurol* 2009; **66**:858–861.
7 McDannold N, Clement GT, Black P, Jolesz F, Hynynen K. Transcranial magnetic resonance imaging-guided focused ultrasound surgery of brain tumors: initial findings in 3 patients. *Neurosurgery* 2010; **66**:323–332, discussion 332.
8 Yoo SS, Bystritsky A, Lee JH, Zhang Y, Fischer K, Min BK, *et al.* Focused ultrasound modulates region-specific brain activity. *Neuroimage* 2011; **56**:1267–1275.
9 Min BK, Bystritsky A, Jung KI, Fischer K, Zhang Y, Maeng LS, *et al.* Focused ultrasound-mediated suppression of chemically-induced acute epileptic EEG activity. *BMC Neurosci* 2011; **12**:23.

10 Yang PS, Kim H, Lee W, Bohlke M, Park S, Maher TJ, *et al*. Transcranial focused ultrasound to the thalamus is associated with reduced extracellular GABA levels in rats. *Neuropsychobiology* 2012; **65**:153–160.
11 Min B-K, Yang PS, Bohlke M, Park S, Rvago D, Maher TJ, *et al*. Focused ultrasound modulates the level of cortical neurotransmitters: potential as a new functional brain mapping technique. *Int J Imaging Syst Technol* 2011; **21**:232–240.
12 Yoo SS, Kim H, Min BK, Franck E, Park S. Transcranial focused ultrasound to the thalamus alters anesthesia time in rats. *Neuroreport* 2011; **22**:783–787.
13 Kim H, Taghados SJ, Fischer K, Maeng LS, Park S, Yoo SS. Noninvasive transcranial stimulation of rat abducens nerve by focused ultrasound. *Ultrasound Med Biol* 2012; **38**:1568–1575.
14 Kim H, Park MA, Wang S, Chiu A, Fischer K, Yoo SS. PET/CT imaging evidence of FUS-mediated (18)F-FDG uptake changes in rat brain. *Med Phys* 2013; **40**:033501–033510.
15 Kim H, Chiu A, Park S, Yoo SS. Image-guided navigation of single-element focused ultrasound transducer. *Int J Imaging Syst Technol* 2012; **22**:177–184.
16 Duck FA. Medical and non-medical protection standards for ultrasound and infrasound. *Prog Biophys Mol Biol* 2007; **93**:176–191.
17 Fonoff ET, Pereira JF Jr, Camargo LV, Dale CS, Pagano RL, Ballester G, *et al*. Functional mapping of the motor cortex of the rat using transdural electrical stimulation. *Behav Brain Res* 2009; **202**:138–141.
18 King RL, Brown JR, Newsome WT, Pauly KB. Effective parameters for ultrasound-induced in vivo neurostimulation. *Ultrasound Med Biol* 2012; **39**:312–331.
19 Younan Y, Deffieux T, Larrat B, Fink M, Tanter M, Aubry JF. Influence of the pressure field distribution in transcranial ultrasonic neurostimulation. *Med Phys* 2013; **40**:082902.
20 Hertzberg Y, Volovick A, Zur Y, Medan Y, Vitek S, Navon G. Ultrasound focusing using magnetic resonance acoustic radiation force imaging: application to ultrasound transcranial therapy. *Med Phys* 2010; **37**:2934–2942.
21 Schweizer R, Voit D, Frahm J. Finger representations in human primary somatosensory cortex as revealed by high-resolution functional MRI of tactile stimulation. *Neuroimage* 2008; **42**:28–35.
22 Hira R, Honkura N, Noguchi J, Maruyama Y, Augustine GJ, Kasai H, *et al*. Transcranial optogenetic stimulation for functional mapping of the motor cortex. *J Neurosci Methods* 2009; **179**:258–263.
23 Berg RW, Kleinfeld D. Vibrissa movement elicited by rhythmic electrical microstimulation to motor cortex in the aroused rat mimics exploratory whisking. *J Neurophysiol* 2003; **90**:2950–2963.
24 Pascual-Leone A, Valls-Sole J, Wassermann EM, Hallett M. Responses to rapid-rate transcranial magnetic stimulation of the human motor cortex. *Brain* 1994; **117 (Pt 4)**:847–858.
25 Ostrow LW, Suchyna TM, Sachs F. Stretch induced endothelin-1 secretion by adult rat astrocytes involves calcium influx via stretch-activated ion channels (SACs). *Biochem Biophys Res Commun* 2011; **410**:81–86.